

## Stick-slip dynamics as a probe of frictional forces

M. G. ROZMAN(\*), M. URBAKH and J. KLAFTER

*School of Chemistry, Tel Aviv University - 69978 Tel Aviv, Israel*

(received 27 February 1997; accepted in final form 17 June 1997)

PACS. 68.15+e – Liquid thin films.

PACS. 46.30Pa – Friction, wear, adherence, hardness, mechanical contacts, and tribology.

PACS. 05.45+b – Theory and models of chaotic systems.

**Abstract.** – In this letter we investigate the nature of relaxation in a model system which consists of a chain of particles that interact with two periodic potentials which represent two confining plates, one of which is externally driven. We find that the relaxation of the “slip” part between two “stick” events in the stick-slip time series may display more than one characteristic time scale. Similar relaxation patterns are observed also in the case of a single particle located between the plates. The different relaxation times are shown to be related to a velocity-dependent effective frictional force felt by the driven plate, and their actual observation is dictated by the experimental conditions.

*Introduction.* – Much attention has been recently devoted to the understanding of the origin and nature of stick-slip motion in systems of confined liquids [1], [2]. Different theoretical models have been proposed to account for this type of motion, including spring-block models [3], chains adsorbed on a substrate [4], melting-freezing mechanism [5]-[7] and an embedded particle model [8], [9]. However, only few studies have focused on the time-dependent relaxation patterns of the “slip” part between two successive “stick” events in this regime. The latter may help unravel some interesting processes related to boundary lubrication, which are otherwise hidden due to the macroscopic nature of the probing methods.

Experimentally, it has been observed [10] that, under overdamped conditions, “slip” relaxation manifests more than one characteristic time scale. Typically a sharp decrease at early times is followed by a tail of slow decay. Phenomenological theoretical studies [5], [6] have suggested that the details of the relaxation really depend on the experimental conditions (underdamped or overdamped) and have related the stick-slip behavior to a dynamical phase transition [5] or to a velocity-dependent frictional force [6].

In this letter we investigate relaxation patterns in the stick-slip regime. We introduce a *microscopic model* which leads to the observed experimental behavior and to predictions that are amenable to experimental tests. The results of our numerical calculations are interpreted in term of a coarse-grained picture [9] of an effective frictional force. We emphasize the effect

---

(\*) Permanent address: Institute of Physics, Riia 142, EE2400 Tartu, Estonia.

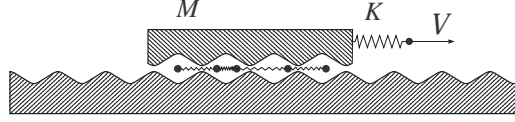


Fig. 1. – Schematic sketch of the model geometry.

of the experimental conditions on the observed behavior, and obtain an explicit dependence on the value of the spring constant.

*The model.* – We have extended the model [8], [9] of a single particle that interacts with two periodic potentials representing two confining plates, one of which is externally driven, to include an embedded chain of particles (fig. 1). Consider a one-dimensional system of two rigid plates and a chain of particles embedded between them. The top plate of mass  $M$  is pulled by a linear spring with a spring constant  $K$  connected to a stage which moves with a velocity  $\mathcal{V}$ .

The equations of motion for the top plate and chain particles are

$$M\ddot{X} + \sum_{i=1}^N \eta(\dot{X} - \dot{x}_i) + K(X - \mathcal{V}t) + \sum_{i=1}^N \frac{\partial U(x_i - X)}{\partial X} = 0, \quad (1)$$

$$m\ddot{x}_i + \eta\dot{x}_i + \eta(\dot{x}_i - \dot{X}) + \sum_{j \neq i} \frac{\partial V(x_i - x_j)}{\partial x_j} + \frac{\partial U(x_i)}{\partial x_i} + \frac{\partial U(x_i - X)}{\partial x_i} = 0, \quad (2)$$

where  $N$  is the number of particles in the chain,  $x_i$  ( $i = 1, \dots, N$ ) and  $X$  are the coordinates of chain particles and the top plate, respectively,  $m$  is the mass of each particle. The second term in eq. (1) and the second and the third terms in eq. (2) describe the dissipative forces between the particle and the plates, which are proportional to their relative velocities. These terms account for dissipation which arises from interaction with phonons and/or other excitations. The third term in eq. (1) is the driving force due to the stage motion. The remaining terms originate from the spatially periodic interaction between the particle and the plates,  $U(x)$ , and from the inter-particle interaction within the chain,  $V(x_i - x_j)$ . There is no direct interaction between the plates. In the present work we choose  $U(x) = -U_0 \cos(2\pi x/b)$ , where  $b$  is the spatial period of the particle-plate interaction potential; the inter-particle potential is assumed to be harmonic with nearest-neighbor interactions only,  $V(x_i - x_{i\pm 1}) = k(x_i - x_{i\pm 1} \mp a)^2/2$ . Here  $k$  is the elastic chain constant, and  $a$  is the equilibrium spacing between particles in a free chain. The model resembles the dissipative dynamics of the Frenkel-Kontorova model [11]. However, here the overdamped condition is on the top plate motion rather than on the chain [11].

Let us introduce dimensionless variables and parameters: the coordinate  $y = x/b$  and the time  $\tau = \omega t$ , where  $\omega = (2\pi/b)\sqrt{U_0/m}$  is the frequency of the small oscillations of the particle in the minima of the potential  $U(x)$ ;  $\gamma = \eta/(m\omega)$ , which is a dimensionless friction constant,  $\epsilon = m/M$ , the ratio of particle and plate masses,  $\alpha = \Omega/\omega$ , the ratio of frequencies of the free oscillations of the top plate  $\Omega = \sqrt{K/M}$  and the particle,  $\delta = (b - a)/b$ , the misfit of the substrate and chain periods, and  $\rho = (\omega_{\text{ch}}/\omega)^2$ , the ratio of the frequencies related to interparticle and particle-plate interactions; here  $\omega_{\text{ch}} = \sqrt{k/m}$  is the characteristic frequency of the chain.

The extension of the single-particle model [8], [9] to a chain adds two new parameters:  $\delta$  and  $\rho$ . The parameter  $\delta$  describes the competition between the chain and potential periodicities and  $\rho$  is the measure of the relative strength of the particle-particle and particle-potential interactions.

In the limits  $\delta = 0$  and  $\rho \ll 1$  or  $\rho \gg 1$  the problem reduces to the single-particle picture, where the case  $\rho \rightarrow 0$  corresponds to  $N$  independent particles and the case  $\rho \gg 1$  to a rigid chain which acts as a single particle.

The chain model introduced above exhibits similar behavior to the one previously observed in the single-particle model [8], [9]. Again the motion of the top plate, which is the experimental observable, shows stick-slip, intermittent and sliding regimes. Here, however, we notice vibrational fluctuations typical of the chain which superimpose on the corresponding single-particle behavior. Generally, the stick-slip dynamics of the chain model is characterized by a chaotic behavior of the top plate and the embedded particles. In this letter we focus only on the range of low stage velocities, where the motion is close to periodic.

*Results.* – We concentrate on the stick-slip regime typical of low driving stage velocities, and analyze a time window which corresponds to “slip” motion between two “stick” events. Namely, just as the top plate overcomes the static friction and starts moving, dissipation sets in and the plate relaxes toward another stick event. This slip relaxation pattern depends on the conditions under which the stick-slip motion is being studied. In the present work we consider the *overdamped* case, where the characteristic slip time is much longer than the response time of the mechanical system  $\sim 2\pi\sqrt{M/K}$ . The overdamped regime is realized experimentally if the spring constant  $K$  is sufficiently weak, and/or if the friction constant  $\eta$  is large. In numerical calculations we use the following values of parameters:  $\epsilon = 1/120$ ,  $\gamma = 0.3$ ,  $N = 15$ ,  $\delta = 0.1$ ,  $\rho = 1.0$ .

Figure 2(a) displays the time evolution of the spring force during the slip motion. One clearly notices more than one time scale in the relaxation process. We divide the slip part into two intervals:  $t_0 < t < t_1$  and  $t_1 < t < t_s$ , as marked in the figure. Following in time the velocity of the top plate (fig. 2(b)) re-emphasizes the existence of two temporal behaviors. Figure 2(b) clearly demonstrates that in the time range  $t_0 < t < t_1$  the velocity drops abruptly, and in the range  $t_1 < t < t_s$  the velocity relaxes slowly towards the stage velocity. In the second time range the amplitude of the velocity oscillations is of order of the average velocity. The two behaviors observed for the spring force and the top plate velocity appear also in the properties of the chain. For instance, the chain length, (fig. 2(c)), shows two distinctive regimes: strong fluctuations for  $t_0 < t < t_1$  and quasi-periodic oscillations around a stretched state for  $t_1 < t < t_s$ .

Similar features of the top plate motion have been observed also in the case of the single-particle model under overdamped conditions [12]. This is in contrast to underdamped results, where the slip time is shorter and slip motion is characterized by one type of behavior.

In order to provide a coarse-grained picture of the top plate motion, which is the basic observable, we use an approximate description [9] based on separation to “slow” and “fast” motions of the system. We describe the slow system motion in terms of an effective velocity-dependent force that acts on the top plate,

$$M\ddot{X} + F(\dot{X}) + K(X - \mathcal{V}t) = 0. \quad (3)$$

The effective force  $F(\dot{X})$  is calculated by assuming that the top plate moves with constant velocity, and by averaging the potential and dissipative components of the friction over the fast fluctuations of the chain motion. Denoting by  $\langle \dots \rangle$  time averaging, we have

$$F(v) = \left\langle \sum_{i=1}^N \frac{2\pi}{b} U_0 \sin \left[ \frac{2\pi}{b} (x_i - vt) \right] + \eta (v - \dot{x}_i) \right\rangle. \quad (4)$$

In fig. 3 we present the effective force  $F(v)$  which has three different regimes: at high plate velocity,  $v > v_{th}$ , the chain decouples from the plates, and is practically free, moving with

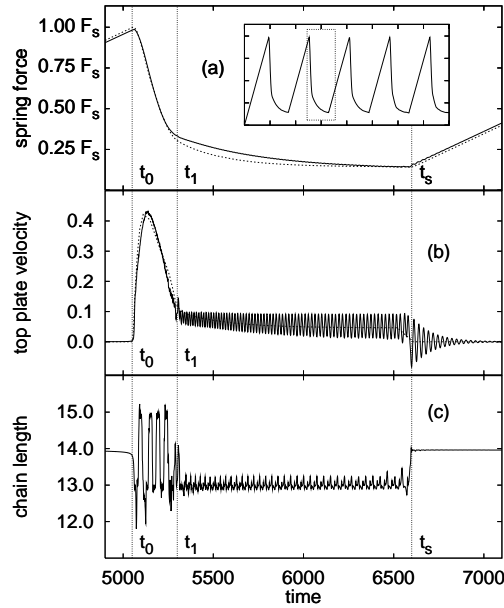


Fig. 2. – Time evolution of the spring force (a), top plate velocity (b), and length of the embedded chain (c), during slip relaxation. Solid lines are the results of simulations, dashed lines in (a) and (b) correspond to the effective force approximation, eqs. (3), (4). The inset shows a stick-slip time series with a window which indicates the time interval presented in (a)-(c). Dimensionless stage velocity  $\mathcal{V}/(\omega b) = 0.046$ , spring constant  $\alpha = 0.015$ .

velocity  $v/2$ . At intermediate velocities,  $v^* < v < v_{th}$ , the chain is trapped by one of the plates and each particle performs small oscillations around the corresponding minimum of the particle-plate interaction potential. At low velocities,  $v < v^*$ , the center mass of the chain again moves with velocity  $v/2$ , but its length strongly fluctuates.

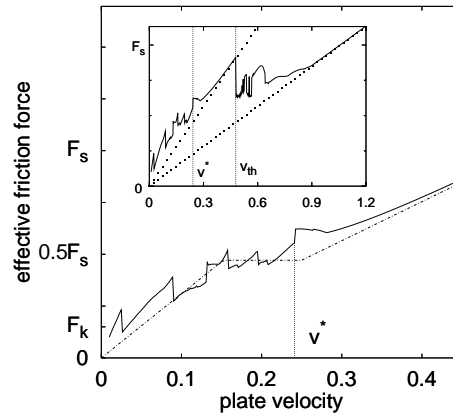


Fig. 3. – Effective frictional force acting on the top plate as a function of plate velocity. The dashed line shows the smoothed force used for the approximate description according to eq. (3). The dotted lines with slopes  $N\gamma$  and  $N\gamma/2$  are presented for reference.

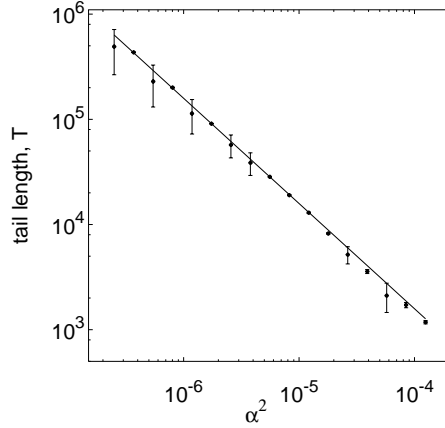


Fig. 4. – Duration of the slow part of slip relaxation as a function of dimensionless spring constant  $\alpha^2 = K/(M\omega^2)$  plotted in double-logarithmic axes. Error bars indicate a dispersion. The straight line with the slope  $-1$  is the best fit to the results of simulations.

The behavior of the effective force in the high-velocity region,  $v > v^*$ , does not depend of the parameters of our model. In the low-velocity region,  $v < v^*$ , we find the following characteristic features of the smoothed frictional force (see fig. 3): a “plateau” for  $v$  close to  $v^*$  and a positive slope of  $F(v)$  for lower velocities. Similar features have been found for other parameter values of the model, however the slope of smoothed  $F(v)$  at small  $v$  and the width of the plateau depend on the microscopic parameters. In order to simulate the motion of the top plate, the effective force, eq. (4), should be supplemented by the static friction  $F_s$  and kinetic friction  $F_k$ . The former is the largest depinning force [9] and the latter is the minimal force necessary to keep the plate sliding at low velocities. The static friction is determined by the potential interaction between the plates and the chain, and the kinetic friction has a dissipative nature. Neither  $F_s$  nor  $F_k$  are included in the effective force found by the time averaging. Estimates [12] give the following values:  $F_s = 2\pi U_0 N/b$  for static friction, and  $F_k \simeq 8\eta N \sqrt{U_0/M}/\pi$  for kinetic friction, which agree with the results of the numerical simulations.

Velocity-dependent forces with features similar to those found here have been postulated to mimic the motion of the top plate in stick-slip experiments [10], [6]. Here we calculate  $F(v)$  directly from the model. In fig. 2 we fit the spring force and top plate velocity, obtained through the solution of eq. (3), to the solution of the model, eqs. (1)-(2).

Introducing the effective force  $F(v)$  makes it possible to relate the two time intervals in slip relaxation (fig. 2) to the nature of  $F(v)$ . Basically, the relaxation pattern should depend on the maximum value of the velocity reached by the top plate. The latter increases with the decrease of the spring constant  $K$ . For our choice of parameters the maximum of the plate velocity lies in the range  $v^* < v_{\max} < v_{\text{th}}$ . The relaxation process spans velocities smaller than  $v_{\max}$ , and therefore probes only those phases that correspond to  $v < v_{\text{th}}$ . Namely, only two regimes are to be expected. Indeed the initial part of the slip relaxation (or top plate velocity) results from the frictional force in the range  $v^* < v < v_{\text{th}}$ , and the longer time relaxation results from  $F(v)$  in the range  $v < v^*$ . Additional support to this picture comes from calculating the trajectories of the chain which show motion with  $\dot{X}/2$  for  $t_0 < t < t_1$  and  $\dot{X}$  for  $t_1 < t < t_s$ . This is in agreement with the results found for the corresponding regimes of the velocity-dependent force  $F(v)$ . The amplitude of the variation of the spring force during slip relaxation equals  $F_s - F_k$ . Both the time dependence and the amplitude of the slip relaxation predicted here are consistent

with the experimentally observed behavior [10].

For other choices of parameters, for which the maximum of the top plate velocity lies in the range  $v > v_{th}$ , the relaxation probes all three characteristic ranges of  $F(v)$  leading to a relaxation pattern with three distinct time scales.

The observed temporal behavior of the slip part depends on how broad the probed range of the effective force  $F(v)$  is. This, as mentioned, depends on  $v_{max}$ , which is determined by the experimentally chosen spring constant  $K$ . Namely, by changing the spring constant  $K$  one can control the experimentally observed relaxation pattern of the slip: one, two or three types of relaxation. The weaker  $K$  is, the larger the probed range of  $F(v)$  is.

Another measurable feature that emerges from the current model is the  $K$ -dependence of the “slow” relaxation part, whose origin is in the low-velocity effective force. Although this region of  $F(v)$  is characterized by large fluctuations, we find that solving eq. (3) for a smoothed  $F(v)$  mimics well the slip relaxation presented in fig. 2 (a)-(b). The top plate velocity strongly oscillates at  $t_1 < t < t_s$ , providing “self-averaging” of the effective force. This is the reason why the smoothed force describes well the slip relaxation also in this time interval.

The use of eq. (3) with the smoothed  $F(v)$  shows that a positive slope of  $F(v)$ , such that  $F'(v)^2 > 4KM$ , is essential for the existence of the slow relaxation part. According to the coarse-grained picture the duration of this part of the slip  $T = t_s - t_1$  should be proportional to  $F'(v)/(2KM)$ . The dependence of  $T$  on the spring constant  $K$  found in our simulations (see fig. 4) is in agreement with this conclusion. This result differs from the conclusion in the melting-freezing model [5], where the duration of the slow relaxation interval is determined by the freezing rate  $\tau^{-1}$  (a parameter not needed in our model), and does not depend of  $K$ .

In summary, we presented a detailed investigation of the stick-slip regime, emphasizing the dependence on damping conditions. Thus the analysis of the slip relaxation could help to differentiate among various mechanisms of friction. Our calculations suggest that the effective frictional force could be reconstructed from measurements of slip relaxation.

\*\*\*

The authors would like to thank F.-J. ELMER for fruitful discussions. Financial support for this work by the Israel Science Foundation is gratefully acknowledged. MR acknowledges the support of the Alexander von Humboldt Stiftung and the Estonian Science Foundation under the grant No. 2689.

## REFERENCES

- [1] YOSHIKAWA H., MCGUIGGAN P. and ISRAELACHVILI J., *Science*, **259** (1993) 1305.
- [2] REITER G., DEMIREL L. and GRANICK S., *Science*, **263** (1994) 1741.
- [3] CARLSON J. M., LANGER J. S. and SHAW B. E., *Rev. Mod. Phys.*, **66** (1994) 657.
- [4] BRAIMAN Y., FAMILY F. and HENTSCHEL G., *Phys. Rev. E*, **53** (1996) R3005.
- [5] CARLSON J. M. and BATISTA A. A., *Phys. Rev. E*, **53** (1996) 4153.
- [6] PERSSON B. N. J., *Phys. Rev. B*, **50** (1994) 4771.
- [7] THOMPSON P. A., ROBBINS M. O. and GREST G. S., *Israel J. Chem.*, **35** (1995) 93.
- [8] ROZMAN M. G., URBAKH M. and KLAFTER J., *Phys. Rev. Lett.*, **77** (1996) 683.
- [9] ROZMAN M. G., URBAKH M. and KLAFTER J., *Phys. Rev. E*, **54** (1996) 6485.
- [10] BERMAN A. D., DUCKER W. A. and ISRAELACHVILI J. N., *Langmuir*, **12** (1996) 4559.
- [11] FLORIA L. M. and MAZO J. J., *Adv. Phys.*, **45** (1996) 505.
- [12] ROZMAN M. G., URBAKH M. and KLAFTER J., to be published.